

VELOCITY FIELDS AND THEIR VARIATION IN THE TWO-DIMENSIONAL  
FORCED PLUME WITHOUT AND WITH A VERTICAL WALL NEARBY

By

Jiro Yoshida\* and Yutaka Nagata

Geophysical Institute, University of Tokyo, Tokyo 113, Japan

\*Present Address: Department of Marine Environmental Science and  
Technology, Tokyo University of Fisheries, Tokyo 108, Japan

SYNOPSIS

The velocity fields and their variation in the two-dimensional forced plumes were measured by using hydrogen bubble technique. The experiments were done mainly for the single plume experiments with and without wall. The ensemble averaged horizontal profile of the observed vertical velocity can be regarded as Gaussian, except just near the vertical wall, but the instantaneous profile of the vertical velocity has a sharpened and pointed peak. The peak of the instantaneous velocity profile vibrates randomly with periods of several seconds around the peak of the averaged velocity profile, and this vibration of the instantaneous profile seems to produce the Gaussian profile in the averaged velocity field. The nature of fluctuating velocity is also analyzed, and the manner of the subsidence of the fluctuation near the wall is discussed.

INTRODUCTION

In the previous papers (Yoshida and Nagata (7); Yoshida (8)), interactions between two two-dimensional forced plumes having the same intensity (dual plume) were discussed. When two plumes are ejected vertically downward adjacent to each other, first they do not interact each other and evolve vertically downward like an ordinary single plume without another plume nearby. But in the next stage, they tend to be deflected towards each other slowly at first and rapidly next. Eventually, they reach a quasi-steady state and merge into one plume at the depth which is determined by the flow rate, the density difference between plume and ambient waters and the distance between the two slots of injection. Such time evolution of dual plume may be mostly simulated by replacing the plane of symmetry with a vertical solid wall. However, the deflection angle of the plume axes in the quasi-steady state is significantly larger in the case where a single plume is ejected near a solid wall. The mechanism of time evolution of dual plume and the reason why such difference occurs in the quasi-steady state if the plane of symmetry is replaced with a solid wall were discussed qualitatively in the previous papers. In these discussions, however, it is suggested that the entrainment process into plume is modified between these two cases, and such modification must be due to change in the structure of the velocity field in and near the plume, depending on the presence of the wall or another plume nearby.

The entrainment process into plume is considered to be closely related to the structure of organized motion from flow visualization and simultaneous multi-point measurements of velocity and/or buoyancy fields (e.g. Kotsovinos and List (4), Chen and Rodi (1), Murota et al. (5)). In the previous investigations, however, the spacing of the measurement points were rather coarse because of the limitation of the size of the probe, of the interaction among probes and so on. And it is also difficult to obtain the instantaneous velocity field, which can directly inform the structure of the organized motion.

By using hydrogen bubble technique, we can obtain the instantaneous velocity field at very close spacing measurement points, and by comparison of instantaneous

profile and mean profile, information of the fluctuation in velocity is also obtained (see, for example, Grass(2)). The motivation of the experiments reported in this paper is to clarify the mechanism of the phenomena mentioned above, and to give the quantitative discussions through the measurements of instantaneous and mean velocity fields in and near the plume by hydrogen bubble technique. The experiments were done for two cases; one is a single plume experiment without a vertical wall nearby, and the other is a single plume experiment with a vertical wall nearby. The velocity measurements were conducted only at a level beneath the depth where the plume axis hits the vertical wall.

#### EXPERIMENTAL PROCEDURE

A lucite tank of 200cm long, 100cm high and 20cm wide was used. For the single plume experiment without vertical wall (see Fig. 1) a narrow channel of

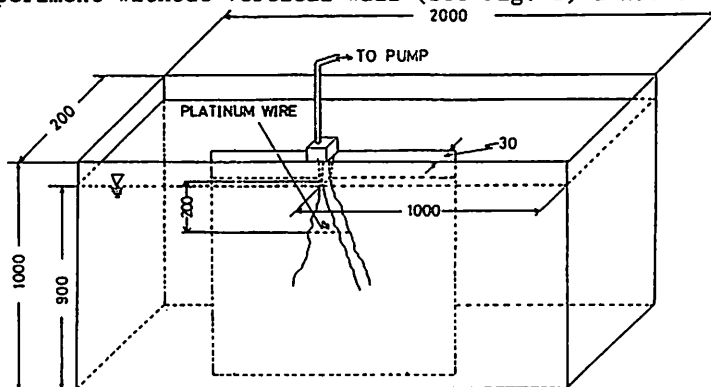


Fig. 1 Schematic view of the experimental apparatus for the single plume experiment without wall. Numbers in the figure indicate length in mm

100cm and 3cm wide was formed in the center part of tank by placing lucite plate vertically in the tank. For the case of single plume experiment with vertical wall, the separation plate was shifted towards right so that its edge is attached to the side wall of the tank, and a narrow channel was formed in the right half of the tank. The tank was filled with fresh water of density  $\rho_1(1.000\text{gr/cm}^3)$  to the height of 90cm before each experiment. Salt water of density  $\rho_2(1.027\text{gr/cm}^3)$  was supplied at the constant velocity of 8.4cm/sec through the slot. The thickness of boundary layer developed on both side of the wall of channel is estimated about 0.5cm from the traverse of the hot film probe to the direction across the channel. Therefore, the effect of the boundary layer can be negligible in the present experiment. The slot consists of two vertical lucite plates and the opening of which was located just at the water surface at the beginning of each experimental run. The opening of the slot is 0.1cm  $\times$  3.0cm. Initial densimetric Froude number is 5.2 for both experiments. Ejection velocity was calculated from the velocity distribution in the feeding tube, which has circular cross section. Velocity distribution in the tube was measured by Laser Doppler Velocimeter. The position of the slot was at the center for the single plume experiment without wall as seen in Fig. 1, and 10cm apart from the side wall for the single plume experiment with wall.

The typical deflection angle of the plume axis in the quasi-steady state for these experimental parameters is about 64 degrees for the single plume case with wall (Yoshida and Nagata(7)). Therefore, it is estimated that the depth where the plume axis hits the vertical wall is about 5cm for the single plume case.

In order to obtain the velocity field and its variation in and near the plume, the hydrogen bubble technique was used. A fine platinum wire of 50  $\mu\text{m}$  diameter was placed at the center of the channel and stretched horizontally at the level 20cm below the slot opening (the water surface) and used as cathode. The section of the wire passing through the plume portion was insulated, leaving gaps of approximately 1mm, by paint spraying through comb mask. Anode plate was placed on the bottom of the tank. A square wave of 0.03sec interval pulsed voltage of 50 volts was fed and fine hydrogen bubbles generated on the wire by electrosis were

used as flow tracers. BOLEX medium speed motion camera was used to photograph the bubbles, and photograph was taken at 1/32 sec interval. Typical features of bubble tracers leaving the wire are shown in Fig. 2. And the visual configuration of the plume without and with wall are shown in Fig. 3a and 3b, respectively. Note that the large scale eddies such as A and B in the Fig. 3a appeared in plume.

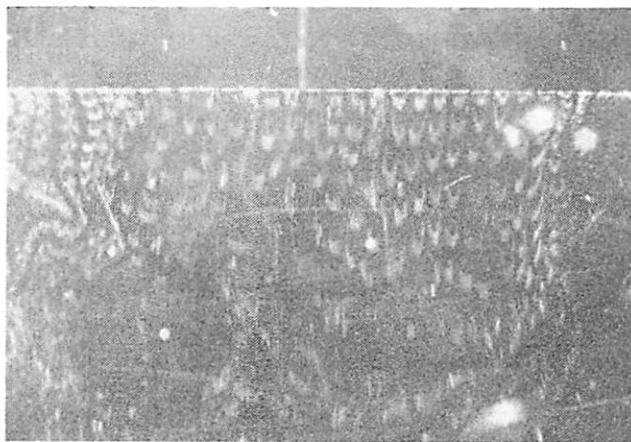


Fig. 2 An example of photographed bubble tracers(single plume experiment without wall). Vertical white belt in the figure shows the position of slot

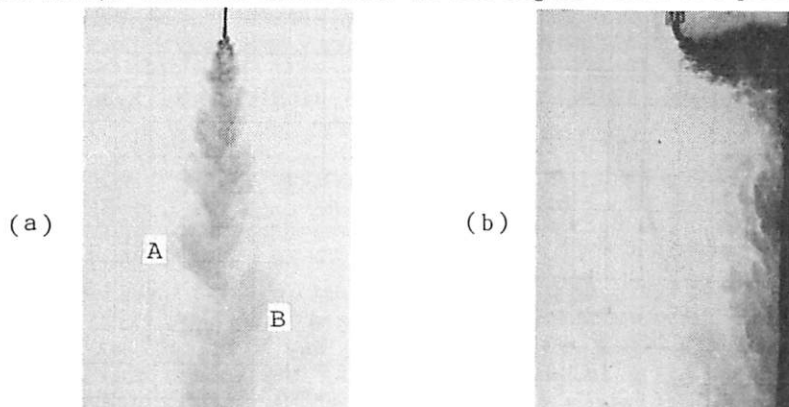


Fig 3 Visual configuration of the plume for the case without wall(a) and with wall(b). The water of plume is colored by dye

The vertical and horizontal velocities along the horizontal line a little below the platinum wire were determined by measuring travel distance of a particular block comparing the photographs taken successively. The depth of measurement was more than 70 wire diameters below the wire so as to avoid the effect of wake of wire and a limit of error in velocity measurement by this method is approximately under 10% (Grass(2)).

Velocity measurements were conducted during about 20 sec after the plume had achieved its quasi-steady state. The velocity data were obtained spatially at an interval of 1mm along the horizontal line. The numbers of data are more than 500 for almost all points (minimum number is 178). Examples of the instantaneous vertical and horizontal velocity profiles are shown in Fig. 4 with open and solid circles, respectively.

For each experimental run, the instantaneous vertical and horizontal velocity components  $u(y,t)$  and  $v(y,t)$  are divided into mean time average velocity components  $\bar{u}(y)$  and  $\bar{v}(y)$  and fluctuating components  $u'(y,t)$  and  $v'(y,t)$  by

$$\begin{aligned} u(y,t) &= \bar{u}(y) + u'(y,t) \\ v(y,t) &= \bar{v}(y) + v'(y,t) \end{aligned} \quad (1)$$

where  $t$  is the time and  $y$  is the horizontal co-ordinate along the observation line

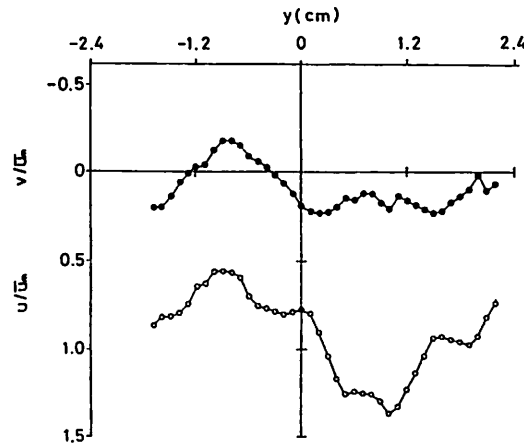


Fig. 4 An example of the instantaneous vertical( $\circ$ ) and horizontal( $\bullet$ ) velocity profile. The profiles are normalized by the maximum velocity  $\bar{u}_m = 6.5 \text{ cm/sec}$  in the averaged vertical velocity profile. Downward and right hand velocity are taken positive measured from the plane of symmetry or from the face of the solid wall.

In preliminary experiments, the level of the platinum wire was varied to 5, 10 and 15 cm below the level of the slot opening. However, the data obtained only at the level of 20 cm are dealt with in this paper, because the horizontal velocity components at the other levels are too strong and changeable and the hydrogen bubbles hardly form clear blocks except for the single plume experiments without wall.

#### TIME AVERAGED STRUCTURES AND INSTANTANEOUS VELOCITY PROFILES

##### *Single Plume without Wall*

The time averaged velocity profiles of vertical and horizontal components along the horizontal line are shown in Figs. 5a and 5b, respectively, for the case when a single plume is ejected freely without any vertical wall nearby. The profile presented in Fig. 5 is given by averaging the values obtained at same  $|y|$  on the the right and left sides of the center, though a little asymmetry is seen in our experiment.

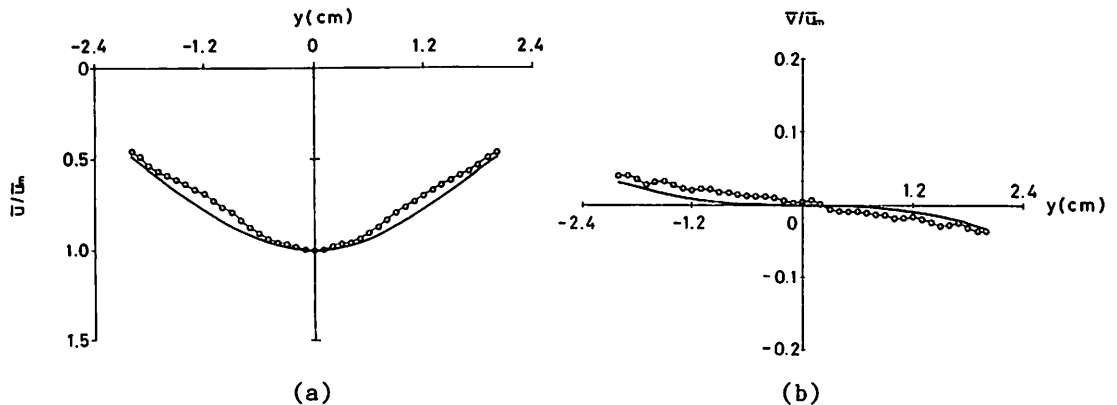


Fig. 5 Averaged profile of the vertical(a) and horizontal(b) velocity component for the case without wall. Gaussian profile obtained by Kotsovinos and List (4) and calculated horizontal profile from Gaussian profile are presented in solid line.  $\bar{u}_m = 6.5 \text{ cm/sec}$

Kotsovinos and List(4) also measured the profile of the vertical velocity component across the two-dimensional forced plume by using LDV, and gave a Gaussian velocity profile;

$$\bar{u}(x,y)/\bar{u}_m(x)=\exp(-73y^2/x^2) \quad (2)$$

where  $x$  is the distance along the plume axis measured from the slot opening,  $\bar{u}_m(x)$  the mean vertical velocity on the plume axis at  $x$ . The velocity profile obtained by substituting  $x=20\text{cm}$  in Eq. 2 is also shown in Fig. 5a with solid line. The profile obtained in our experiment has a little sharper peak than that given by Kotsovinos and List(4). The difference may be attributable to the short averaging time (The typical averaging time is 16 sec in our experiment, while that used by Kotsovinos and List(4) is about 200sec). A part of the difference may come from the sharpness of the peak in the instantaneous profile discussed below.

The profile of the horizontal velocity component may be derived from Eq. 2 by using the equation of continuity. This gives

$$\bar{v}(x,y)/\bar{u}_m(x)=p\exp(-73p^2)-\int_0^p \exp(-73p^2)dp \quad (3)$$

where  $p=y/x$ . The curve corresponding to (3) is also shown in Fig. 5b. The obtained data points are aligned along the curve fairly well.

As seen in Fig. 4, the instantaneous profile of the vertical velocity is not so similar to the Gaussian profile, and shows sharp peak near its maximum. To know the typical instantaneous profile, the position of the maximum velocity was determined for each instantaneous profile, and each profile was shifted horizontally so that its maximum velocity is located at  $y'=0$ . Then the averaging was made for all profiles. The typical instantaneous profile thus obtained is shown in Fig. 6(horizontal co-ordinate for typical instantaneous profile is represented by  $y'$ ). It should be noted that the typical instantaneous profile of the vertical

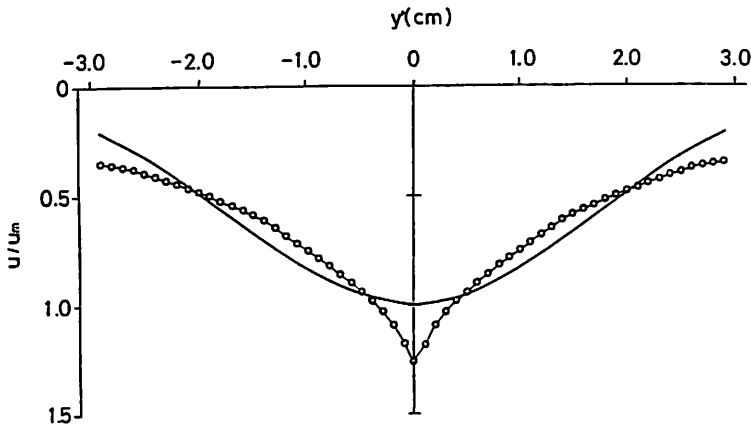


Fig. 6 Typical instantaneous profile of the vertical component for the single plume case without wall.  $\bar{u}_m=6.5\text{cm/sec}$

velocity component has a sharp pointed peak\*, while the time averaged profile can be approximated by Gaussian profile. This means that the position of the maximum velocity of instantaneous profile oscillate somewhat randomly about  $y=0$  and that it produces Gaussian profile in the time averaged sense according to the central limiting theorem.

In Fig. 7 the change of the instantaneous profile of the vertical velocity according to their peak position are shown. These profiles were obtained by averaging the profiles whose maximum velocities are located at  $y=0$ (o), at  $|y|=0.4\text{cm}$ (●), at  $|y|=0.8\text{cm}$ (Δ) and  $|y|=1.2\text{cm}$ (▲), respectively. These profiles also have

\* The sharpness of the peak might be exaggerated in this analysis. The peak would be sharpened if random eddies of small scale have velocity profile having very sharp peak and if some of the vertical velocity maxima in the instantaneous profiles are caused from such random eddies.

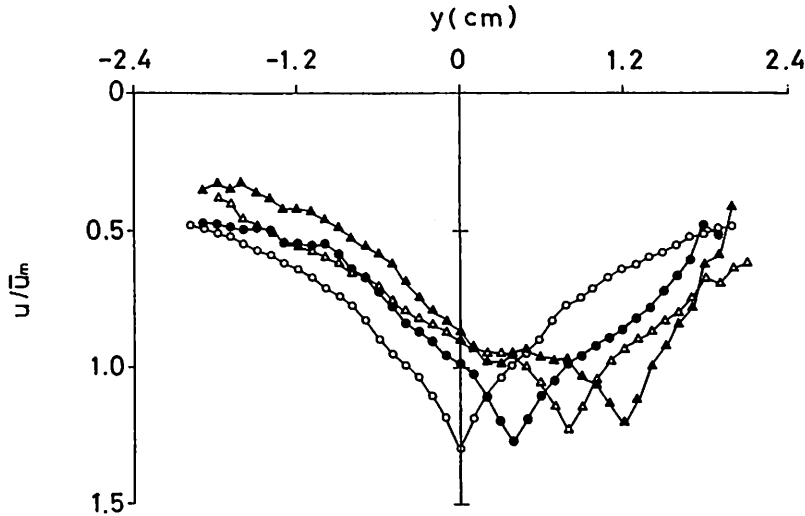


Fig. 7 Change of the instantaneous profile of the vertical velocity component according to their peak position for the case without wall.  $\bar{u}_m = 6.5 \text{ cm/sec}$

sharp peaks near their maximum velocities. Wavy forms sometimes appeared in slope portions seem to be produced because of the limited number of averaging. When the position of the maximum velocity moves apart from the plume axis (the center of the time averaged profile), the slope of the profile at the outer side tends to increase and that at the inner side tends to decrease. It should be noted, however, that the sharpness of the peak near the velocity maximum is almost unchanged for all profiles. Usually, the position of the maximum velocity is easily determined even in the individual instantaneous velocity profiles, and so it will be used later for the analysis of the periodicity of the oscillation of the typical instantaneous profile.

The individual instantaneous profiles of the horizontal velocity component were also shifted so that the positions of the maximum velocity in the corresponding profile of the vertical velocity are located at  $y' = 0$ , and were averaged to get the typical instantaneous profile. The result is shown in Fig. 8. The magnitude

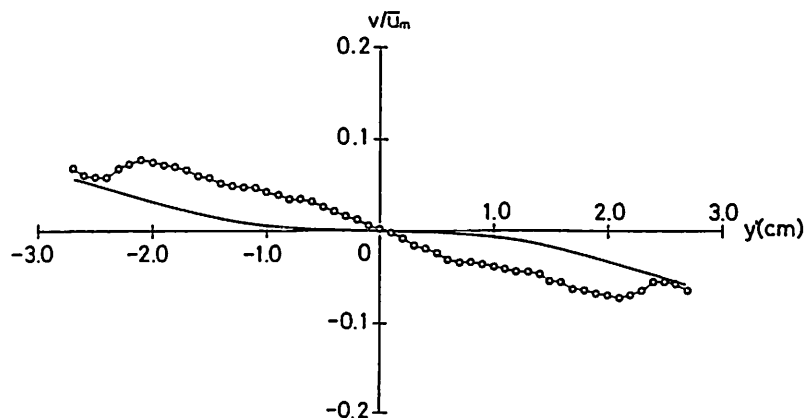


Fig. 8 Typical instantaneous profile of the horizontal component for the case without wall. Solid curve is same as in Fig. 5b.  $\bar{u}_m = 6.5 \text{ cm/sec}$

of the gradient of the curve in the central part of the plume is larger than that in the curve in Fig. 5b. This seems to correspond to the increase in the magnitude of the gradient near the peak in the instantaneous profile of the vertical velocity component as seen in Fig. 6.

From Fig. 3a and 3b we can clearly see that the development of eddies to the direction of the wall is suppressed by the presence of wall. Therefore, in order to know such difference in appearance of plume without and with vertical wall nearby, velocity fields in and near plume with vertical wall nearby are discussed in this section.

The time averaged profiles of the vertical and horizontal components for the case when a single plume is ejected near a vertical wall are shown in Figs. 9a and 9b. The Gaussian profiles of the vertical velocity component given by Eq. 2 are

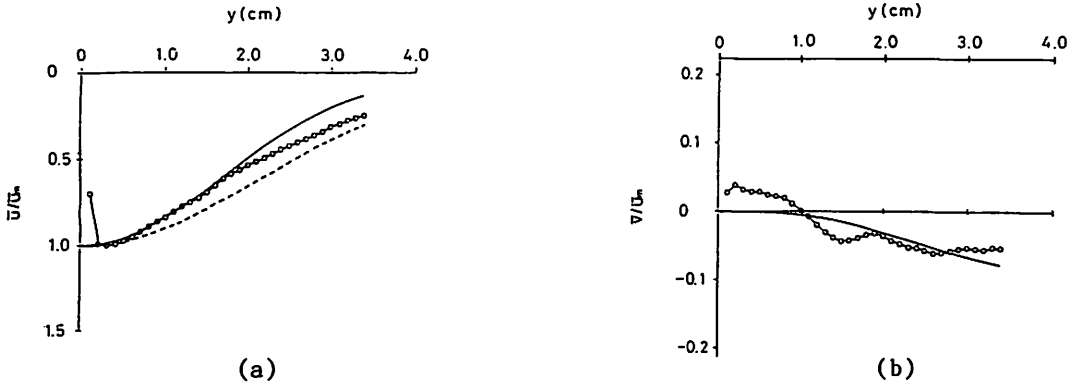


Fig. 9 Averaged Profile of the vertical(a) and horizontal(b) velocity component for the case with wall nearby. The profiles are normalized by the maximum velocity  $\bar{u}_m = 8.4 \text{ cm/sec}$  in the averaged vertical velocity profile.

also given in the figure for  $x=20\text{cm}$  (solid curve) and for  $x=26\text{cm}$  (dashed curve), of which  $20\text{cm}$  is the depth of the level where the measurement was made, and  $26\text{cm}$  is the distance from the slot opening to the measurement level along the oblique plume axis in the upper part along the wall face under the depth where the plume axis hits the wall. Calculated horizontal profile from Gaussian profile for  $x=20\text{cm}$  is shown in Fig. 9b with solid curve. Except very close to the wall and far outside, the measured profile seems to fit the curve for  $x=20\text{cm}$  and be regarded as a Gaussian profile. However, the profile should be compared rather with the curve for  $x=26\text{cm}$ , and it is concluded that the averaged profile produced in our experiments has sharper peak or smaller standard deviation in comparison with the results of Kotsovinos and List (4), just as discussed in the case of the single plume without a vertical wall (see Fig. 5a).

It can be seen in Fig. 9a that the viscous sublayer is developed near the wall and that the maximum vertical velocity appears  $0.3\text{cm}$  apart from the wall face. From the velocity difference of  $5.8\text{cm/sec}$  between  $y=0$  and  $y=0.1\text{cm}$ , we can estimate that the friction velocity  $u_* = \sqrt{\nu / \rho_2 du/dy}$  to be  $0.78\text{cm/sec}$ , where  $\rho_2$  is the density ( $=1.027\text{gr/cm}^3$ ) and  $\nu$  the viscosity of the ejected salt water ( $0.011\text{cm}^2/\text{sec}$  at temperature  $20^\circ\text{C}$ ). The thickness  $y^*$  of the viscous sublayer (the height above which the logarithmic law is applicable for the uniform flow over a flat plate) is given by

$$y^* = 30 \nu / u_* \quad (4)$$

(see, for example, Kline et al. (3)) and is  $0.41\text{cm}$  for our case. The value roughly agrees with the position of the maximum of the vertical velocity component. Thus, the vertical velocity component is strongly influenced by the existence of the wall boundary layer.

The averaged profile of the horizontal velocity component in Fig. 9b shows the outward flow region near the wall. However, this region corresponds to the high velocity region in the vertical velocity component, and the reliability in the estimation of the horizontal component is very limited there. Except this region, the experimental data agree fairly well with the curve based on Eq. 3 for  $x=20\text{cm}$ .

The typical instantaneous profile of the vertical velocity was also calculated as shown in Fig. 10. On the wall side portion of the velocity maximum ( $y' < 0$ ), the number of available data decreases with the increase of  $|y'|$ , So the

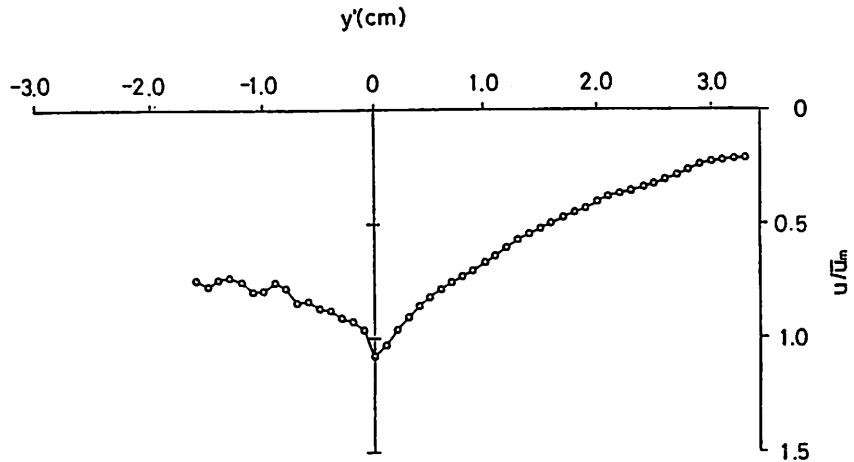


Fig. 10 Typical instantaneous profile of the vertical velocity component for the case with wall nearby.  $\bar{u}_m = 8.4 \text{ cm/sec}$

reliability of the data near the left end of the figure is also limited. It should be noted that the instantaneous profile has a sharp peak even in the single plume case with wall, though the sharpness seems to be a little smaller than that in the single plume case without wall.

For the case when a single plume is ejected freely without wall, the instantaneous velocity profile might be affected by the ejection condition, such as the shape of the slot and the velocity profile in the slot. The observation line discussed in this subsection is located 15cm below the depth where the plume axis hits the wall, and so the plume characteristics there thought to be free from the ejection condition. Therefore, it should be reasonable to conclude that the sharpness of the peak is a common and general feature in the profile of vertical velocity across the plume.

The change of the instantaneous profile of the vertical velocity according to their peak position are shown in Fig. 11. These profiles were obtained by averaging

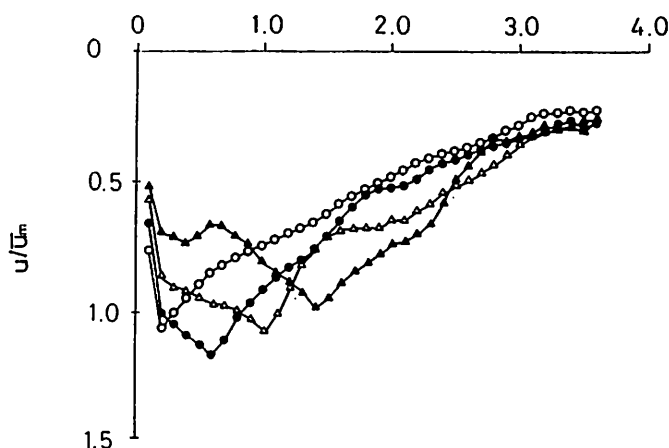


Fig. 11 Change of the instantaneous profile of the vertical velocity component for the case with wall nearby.  $\bar{u}_m = 8.4 \text{ cm/sec}$

ing the profiles whose maximum velocities are located at  $y=0.2 \text{ cm}$  (o),  $y=0.6 \text{ cm}$  (●),  $y=1.0 \text{ cm}$  (Δ) and  $y=1.4 \text{ cm}$  (▲), respectively. The decrease of velocity in the wall side of the velocity maximum is usually smaller than that in the outer side of the maximum. The slope of the profile at the outer side tends to increase when the position of the maximum velocity moves out from the wall face, just like the single plume case without wall.



# TEMPORAL CHANGE OF THE POSITION OF THE INSTANTANEOUS VELOCITY PROFILE

Due to the sharpness of the peak in the instantaneous profile, it is easy to determine the position of the vertical velocity maximum for each instantaneous profile. The temporal variations of the position of the maximum velocity are shown in Figs. 12a and 12b for the single plume case without and with wall, respectively. The fluctuation for the case without wall is somewhat symmetrical

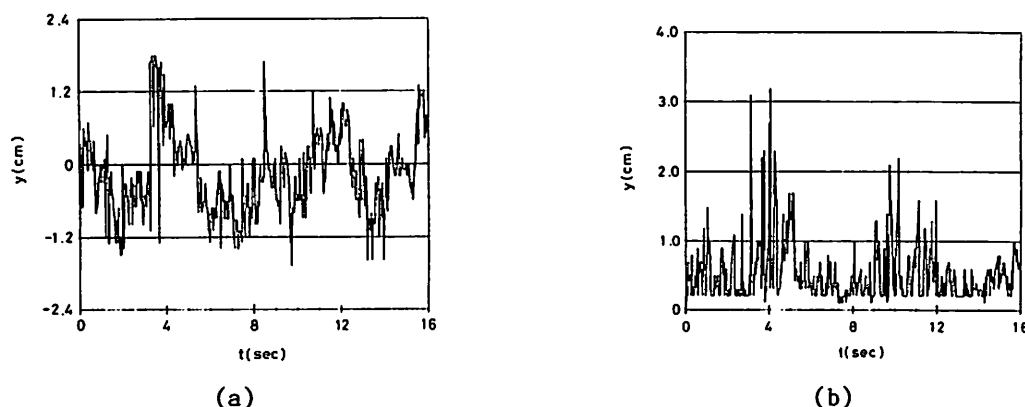


Fig. 12 Temporal variation of the position of the vertical velocity for the case without wall(a) and with wall(b)

about  $y=0$ , while that for the case with wall is confined for  $y>0.1\text{cm}$  (mainly for  $y>0.2\text{cm}$ ) because of the existence of the viscous sublayer near the wall. Both curves exhibit complicated fluctuation characteristics including many components in broad range of frequencies.

Many of the individual velocity profiles of the vertical velocity have several side peaks, though usually the most prominent peak can be easily identified(see Fig. 4). Such side peaks tend to be canceled out in the process of the averaging, and the typical instantaneous profiles in Figs. 6 and 10 have very smoothed side slopes. However, they produce the wavy forms on the side slopes in some of the profiles in Fig. 7 and Fig. 11, because the number of data for averaging is greatly decreased in these cases. In the individual instantaneous profiles, the magnitude of some side peaks may exceed that of the main peak very temporally, and the position of the maximum velocity may shifted abruptly and discretely. Though the used time interval of  $1/32\text{sec}$  is too large and not enough to resolute the high frequency components in Figs. 12a and 12b, typical(or of large amplitude) variations in these figures may be understood as such phenomena occur, and seem to be attributable to random velocity fluctuations.

Besides the high frequency fluctuation, the low frequency fluctuation having the periods of several seconds can be seen both in Figs. 12a and 12b. This fluctuation seems to correspond to meandering in the visual configuration of the plume (see Fig. 3a). The amplitude of the low frequency fluctuation for the case with wall are much smaller than for the case without wall. This implies that the existence of the wall significantly suppresses the meandering of the plume and decreases the magnitude in the position of the instantaneous velocity profile. It should be also noted that the magnitude of the high frequency fluctuation tends to increase when the position of maximum velocity leaves the wall face. The maximum amplitude of the high frequency fluctuation occurs about  $t=4\text{sec}$  in Fig. 12b when the position of the maximum velocity in the profile apparently leaves the wall face.

Spectral analysis of the position (time interval is  $1/32\text{sec}$  and the length of the data is  $16\text{sec}$ ), is shown in Fig. 13. It is clearly seen that the magnitude of the spectral level of fluctuation is greatly diminished for the case with wall not only in low frequency region but also in high frequency region. We can also see that the prominent period of fluctuation is about 4-6 sec for both cases, and it seems to corresponds to the periods of meandering of plume.

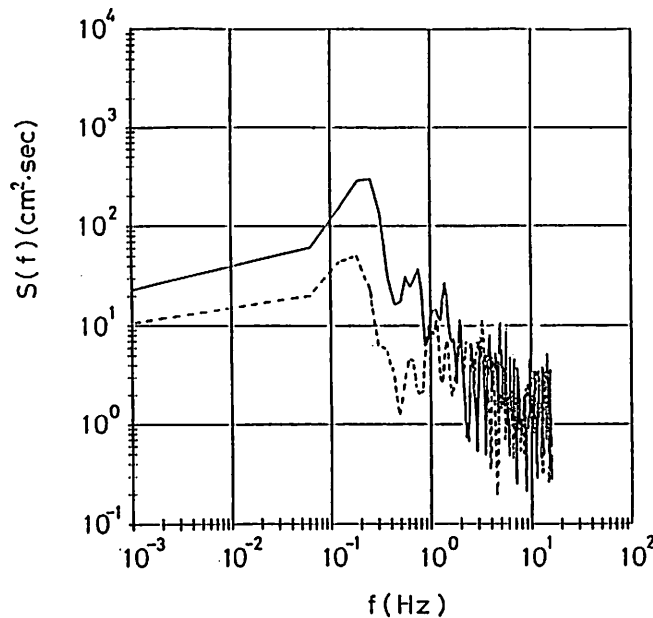


Fig. 13 Spectra of the position of the vertical velocity maximum for the case without wall(solid line) and with wall(dashed line)

#### FLUCTUATION VELOCITY COMPONENTS

The fluctuation velocities  $u'$  and  $v'$  defined by Eq. 1 is discussed in this section. Note that the fluctuation velocity components are not defined as deviations from the typical instantaneous velocity profiles, but as deviations from the time averaged velocity profiles. So some of the characteristics of the fluctuation velocity would be related to the variation of the position of the instantaneous velocity profiles.

##### *Single Plume without Wall*

Correlations between  $u'$  and  $v'$  are shown as scatter diagrams in Figs. 14 (a)  $y=-1.4\text{cm}$ , (b)  $y=-1.0\text{cm}$ , (c)  $y=-0.2\text{cm}$ , (d)  $y=0\text{cm}$ , (e)  $y=0.2\text{cm}$ , (f)  $y=1.0\text{cm}$ , and (g)  $y=1.4\text{cm}$ , respectively for the single plume case without wall. Correlation between  $u'$  and  $v'$  is generally high except near  $y=0$ . The scattering of the data points at  $y=0$  (Fig. 14d) is symmetrical with  $u'$ -axis, and magnitude of the scattering in the direction of  $u'$ -axis is almost the same as that in the direction of  $v'$ -axis. However, when the observation point leaves the plume axis, scattering of the data points becomes of elliptical shape. The major axis of the ellipse is generally deflected anticlockwise for the data taken at  $y<0$  (Figs. 14a through 14c) and clockwise for the data taken at  $y>0$  (Figs. 14e through 14g). To know these characteristics more precisely, the direction of the major axis  $\theta$  is determined by rotating the co-ordinate system ( $v', u'$ ) and by finding the axis along which the variance of the fluctuation velocity has the maximum value\*.

The distribution of the direction  $\theta$  thus obtained is shown in Fig. 15. The value of  $\theta$  shown in the figure is measured anticlockwise from vertical line (note that the  $x$  is taken downwards). The absolute value of  $\theta$  is almost constant within the experimental error except just the plume axis ( $y=0$ ), and  $\theta$  abruptly changes its sign across the plume axis. The characteristics of the distribution can be explainable if the fluctuation velocity is pronounced mainly from the shifting or vibration of the instantaneous velocity profile. If the position

---

\* The similar analysis was made by Nagata (6) in order to obtain its principal direction and long-crestedness of the oceanic waves from the orbital velocity measurements.

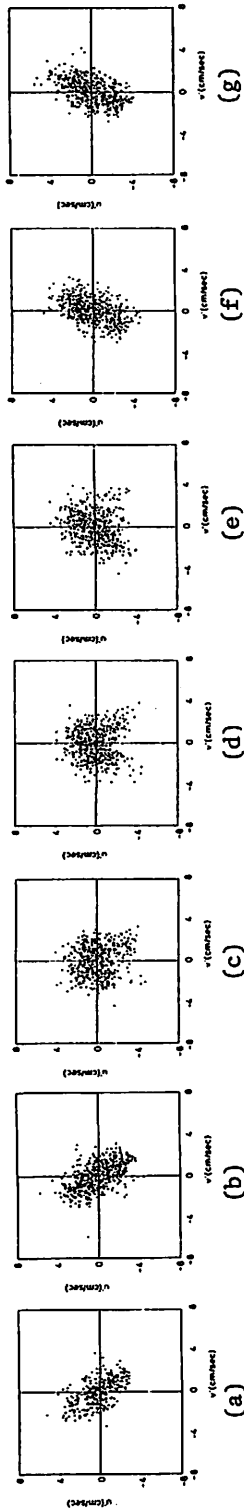


Fig. 14 Scattering diagram of the fluctuation velocity for the case without wall. The position  $y$  is measured from the plume axis towards right

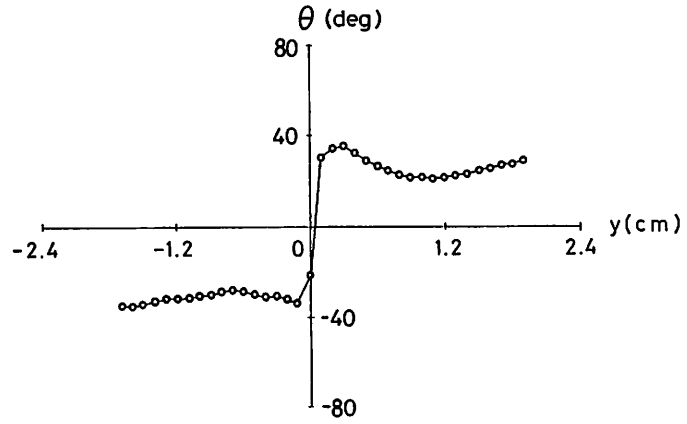


Fig. 15 Distribution of the deflection angle  $\theta$  for the case without wall

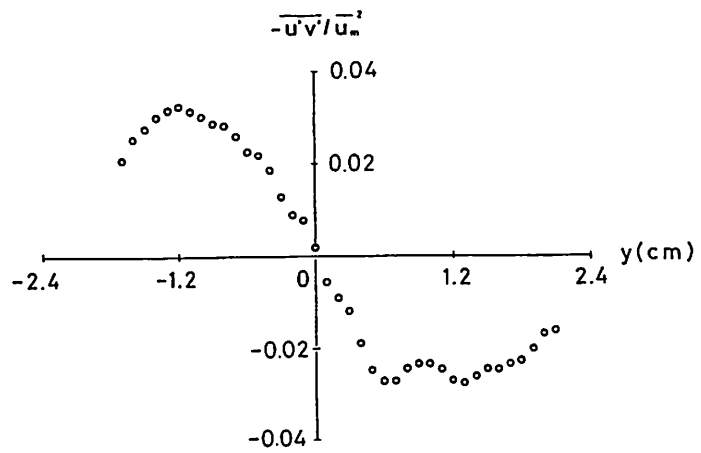


Fig. 16 Distribution of  $-\overline{u'v'}$  for the case without wall.  $\bar{u}_m = 6.5 \text{ cm/sec}$

moves from left to right, downward vertical velocity would be increased at the right hand side of the peak, and would be decreased at the left hand side because of the axial symmetry of the instantaneous vertical velocity profile. While, the horizontal velocity would be increased at both sides, namely, ambient fluid is mainly entrained into plume from left hand side. This means that if the position moves from right to left, ambient fluid is mainly entrained from right hand side. Namely, positive  $\theta$  for  $y > 0$  and negative  $\theta$  for  $y < 0$  means that alternate entrainment process is occurred associate with the weakening of the vertical velocity. In these processes good correlation should be resulted between  $u'$  and  $v'$ , and  $\overline{u'v'}$  should have opposite sign between at right hand side and left hand side of the plume axis (see Fig. 16).

The constancy of the magnitude of  $\theta$  and the very narrow transition near  $y=0$  is somewhat curious. This nature might be attributable to the pointed peak in the instantaneous vertical velocity profile and the decrease of the slope magnitude with increase of the distance from the peak position (see Fig. 6). For large values of  $|y|$ , the position of the maximum velocity hardly pass the observation point and the sign of the  $u'v'$  would be conserved. So the magnitude of  $\overline{u'v'}$  become relatively large even if the magnitude of  $u'v'$  is small. On the contrary, the position of the maximum velocity passes the observation point very frequently for small values of  $|y|$ . The sign of  $u'v'$  would be changed frequently and this results relatively small values of  $u'v'$  even though the magnitude of  $u'v'$  is large. This situation may be seen in the scatter diagram of  $u'$  and  $v'$  near  $y=0$ . The distribution of the data points at  $y=0$  (Fig. 14d) is obliquely elongated in the third and fourth quadrants. The similar nature can be also seen in the distribution at  $y=-0.2\text{cm}$  (Fig. 14c) and  $y=0.2\text{cm}$  (Fig. 14e), though one of the elongated branch is weakened in these figures.

#### Single Plume with Wall nearby

The scatter diagram of the fluctuation velocity for the single plume case with wall are shown for  $y=0.2\text{cm}$ ,  $0.4\text{cm}$ ,  $1.2\text{cm}$  and  $2.0\text{cm}$  in Figs. 17a through 17d,

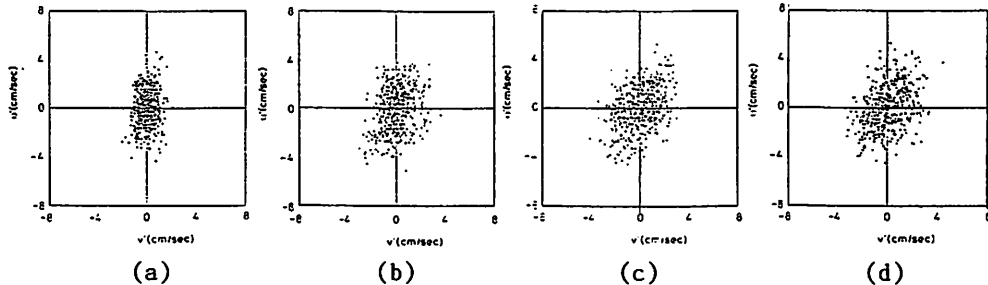


Fig. 17 Scattering diagram of the fluctuation velocity for the case with wall nearby. The position  $y$  is measured from the wall face

respectively. The scattering patterns for  $y > 1.0\text{cm}$  are very similar to those taken for  $y > 1.0\text{cm}$  for the case without wall. For  $y < 1.0\text{cm}$ , we can clearly see that the magnitude of the horizontal component of the fluctuating velocity is suppressed by the presence of wall and diminishes towards the wall face, and the deflection angle of the major axis of the elliptical scattering pattern tends to decrease. This nature is clearly seen from the distribution of the deflection angle  $\theta$ , comparing between that for the case with wall ( $\bullet$ ) and that for the case without wall ( $\circ$ ) in Fig. 18. The decrease of  $\theta$  towards the wall means that alternating entrainment process occurred for the case without wall is suppressed for the case with wall and sufficiently far from wall intermittent entrainment process occurs. Distribution of  $-u'v'$  for the case with wall is shown in Fig. 19. In this figure results for the case without wall is also shown for comparison. It is noted that the decrease in magnitude for the case with wall occurs for the region  $y < 2.0\text{cm}$ , and that this value roughly corresponds to the maximum amplitude of the high frequency fluctuation in the variation of the position of the maximum instantaneous velocity (see Fig. 12a).

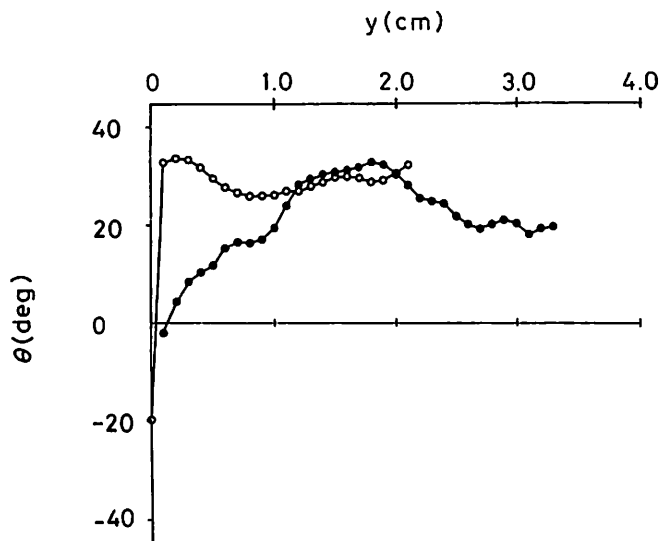


Fig. 18 Distribution of the deflection angle  $\theta$  for the case with wall(●) and without wall(o)

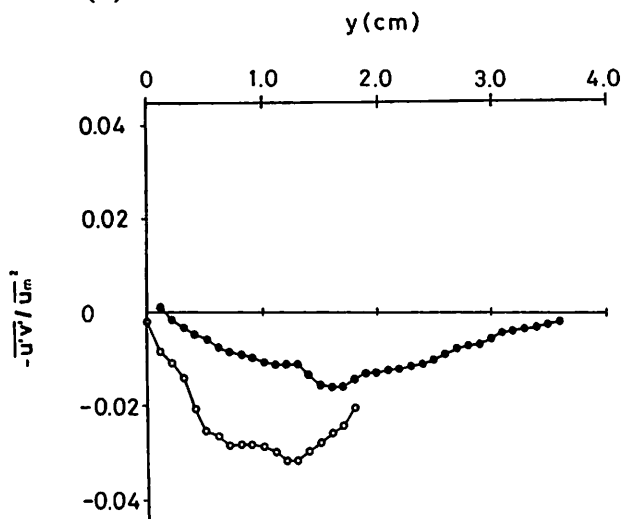


Fig. 19 Distribution of  $-u'v'$  for the case with wall(●) and without wall(o)  
 $\bar{u}_m = 6.5 \text{ cm/sec}$  and  $8.4 \text{ cm/sec}$  for the case without wall and with wall nearby, respectively

#### SUMMARY AND CONCLUSIONS

It is shown that the instantaneous vertical velocity profiles across the plume for the cases without and with wall nearby have a sharp and pointed peak, But the averaged velocity profile can be regarded as Gaussian, except very near the wall for the case with wall. The position of the instantaneous velocity profile vibrates randomly with periods of several seconds about the center of the averaged velocity profile, and seems to produce the Gaussian profile in the averaged vertical velocity field. A good correlation can be found between vertical and horizontal fluctuation velocity for both cases. This high correlation is attributable to the vibration of the position of the instantaneous velocity profiles. And it is found that fluctuation velocity near the wall is subsided because such vibration of the instantaneous velocity profile is prevented by the presence of the wall.

## ACKNOWLEDGMENT

The authors wish to express their heartfelt thanks to Professors Kinjiro Kajiura and Isamu Aida for their guidance and encouragement throughout this study. They also wish to express their thanks to Professors Yusuke Fukushima and Takashi Asaeda for their advice and discussions. Thanks are also extended to Mr. Kiyoshi Kawasaki and Sin'iti Iwasaki for their discussion and helps in this study.

## REFERENCES

1. Chen, C.J. and W. Rodi : Vertical Turbulent Buoyant Jets-A Review of Experimental Data, Pergamon Press, 83pp., 1980.
2. Grass, A.J. : Structural features of turbulent flow over smooth and rough boundaries, J. Fluid Mech., vol.50, pp.233-255, 1971.
3. Kline, S.J., W.C. Reynolds, F.A. Schraub and P.W. Runstadler : The structure of turbulent boundary layers, J. Fluid Mech., vol.30, pp.741-773, 1967.
4. Kotsovinos, N.E. and E.J. List : Plane turbulent jets, Part1, Integral properties, J. Fluid Mech., vol.81, pp.25-44, 1977.
5. Murota, A., K. Nakatsuji and M. Tamai : Structure of organized motion observed in plane forced plume, Proc. 30th Japanese Conf. on Hydraulics, JSCE, pp.649-654, 1986. (in Japanese)
6. Nagata, Y. : The statistical properties of orbital wave motions and their application for the measurement of directional wave spectra, J. Oceanogr. Soc. Japan, vol.19, pp.169-181, 1964.
7. Yoshida, J. and Y. Nagata : The behavior of the two dimensional forced plume ejected near the vertical wall, Coastal Engineering in Japan, vol.22, pp.111-122, 1979.
8. Yoshida, J.: The behavior of a two-dimensional dual forced plume, J. Oceanogr. Soc. Japan, vol.39, pp.317-323, 1983.

## APPENDIX - NOTATION

The following symbols are used in this paper:

$p$	=similarity variable ( $=y/x$ );
$t$	=time
$u$	=instantaneous vertical velocity;
$\bar{u}$	=time averaged vertical velocity;
$u'$	=fluctuation vertical velocity;
$\bar{u}_m$	=time averaged vertical velocity on plume axis;
$u_*$	=friction velocity;
$v$	=instantaneous horizontal velocity;
$\bar{v}$	=time averaged horizontal velocity;
$v'$	=fluctuation horizontal velocity;
$x$	=vertical co-ordinate along the plume axis for the single plume case without wall and along the wall for the single plume case with wall;
$y$	=horizontal co-ordinate along the observation line for mean profile;
$y'$	=horizontal co-ordinate along the observation line for typical instantaneous profile;
$y^*$	=thickness of the viscous sublayer;
$\theta$	=direction of the major axis of $(v', u')$ scattering ellipse;
$\nu$	=molecular viscosity of the water; and
$\rho$	=density of water.